lubricants

MDPI

Article

Tribological Behavior of HNBR in Oil and Gas Field Applications †

Winoj Balasooriya [1,*], Bernd Schrittesser [1], Chao Wang [1], Andreas Hausberger [1], Gerald Pinter [2] and Thomas Schwarz [3]

1 Polymer Competence Center Leoben GmbH, Roseggerstrasse 12, 8700 Leoben, Austria; Bernd.Schrittesser@pccl.at (B.S.); Chao.Wang@pccl.at (C.W.); Andreas.Hausberger@pccl.at (A.H.)
2 Department of Polymer Engineering and Science—Materials Science and Testing of Plastics, Montanuniversitaet Leoben, 8700 Leoben, Austria; gerald.pinter@unileoben.ac.at
3 SKF Sealing Solutions Austria GmbH, 8750 Judenburg, Austria; Thomas.Schwarz@skf.com
* Correspondence: Winoj.Balasooriya@pccl.at; Tel.: +43-3842-429-6232
† This paper is an extended version of our paper published in 6th World Tribology Congress, Beijing, China.

Received: 10 January 2018; Accepted: 11 February 2018; Published: 13 February 2018

Abstract: The common usages of elastomeric components in oil and gas field applications are in dynamic atmospheres; especially sealing appliances that are in relative motion when interacting with surfaces. Therefore, their performance and service life mainly depend on the wear and friction characteristics in use. The objective of this scientific work is to identify the effect of swelling-induced ageing on the tribological properties and surface damage mechanisms of hydrogenated nitrile butadiene rubber (HNBR) in contact with different liquids. Furthermore, the investigation of the co-relation between mechanical properties and surface properties in the tested conditions is indispensable. In the swollen state, deteriorated mechanical properties were observed; however, in de-swollen conditions, the mechanical properties were restored. As far as the surface characterization is concerned, when the HNBR was swollen by a standard IRM 903 solvent, its wear was greater compared with the un-swollen specimen (1.1 times) despite the lower coefficient of friction (COF) (reduced by ~25%) and surface temperature (reduced by ~2.4 °C). In the de-swollen condition, wear was even greater (6 times), but the COF and surface temperature were situated in between those recorded in the swollen and un-swollen conditions. With swelling, greater wear damage and lower COF were observed; higher surface ageing (softness), which eases crack growth, created bigger debris. Under the conditions used, in the de-swollen states, the bulk mechanical properties were almost recovered, in contrast to the surface properties, which were still significantly impaired.

Keywords: elastomeric materials; HNBR; swelling-induced ageing; mechanical and tribological characterization; surface analysis

1. Introduction

Elastomers are a popular class of materials in oil field applications for sealing, down-hole packers, gaskets, etc. due to their soft, nearly elastic, and incompressible nature [1]. Especially, seals prevent the leakage of fluids and/or gas from a machine and contamination of the environment [2]. However, their performance and service life depend on the wear and friction characteristics in use [3]; therefore, tribology (the study of wear, friction, and lubrication) is an important factor for the seal performance and the overall efficiency of a machine [2,3]. It is necessary to reduce the coefficient of friction (COF) and wear rate of rubber composites for better performance [4]. The tribology of rubber is a complex phenomenon and depends mainly on the configuration of the tribo-testing rig, sliding speeds, applied loads, surface properties of the counterpart, sliding mode, contact area, etc. [5].

Wear in rubber materials is expected as a result of two processes: tearing (local mechanical rupture) and smearing (general decomposition of the molecular network to a low molecular weight material) [6,7]. These are affected by crack growth behavior, the mechanical properties of the rubber, chemical ageing, and the thermal conductivity of the composite [8]. Wear mechanisms can be classified as abrasive wear, fatigue wear, and roll formation. Abrasive and fatigue wear occur frequently on harsh and blunt surfaces, respectively, and roll formation occurs on relatively smooth surfaces of the abrading counterpart and for relatively smooth and soft elastomers [8]. Therefore, wear resistance is the ability of a material to resist mechanical actions, such as rubbing, scraping, or erosion, that tend progressively to remove material from its surface, which is related to the structural unit, localized stresses of the rubber, or initial substrate failure due to flaws in the rubber [8]. The viscoelastic nature of elastomers results in shear wave propagation along the surface of rubber during sliding, where it increases the surface area; these waves are known as "Schallamach waves" [8]. Therefore, with increasing applied normal force the wear due to the increased contact area rises [9]. Moreover, adding fillers rather than gum to elastomers seems to increase the abrasion resistance due to increased mechanical properties [10].

Rubber friction is considered to be based on two main components: adhesion and hysteresis behavior. While adhesion creates the stick-slip action between the rubber and the counter surfaces, hysteresis is a bulk phenomenon within the body of the rubber [8,11–13]. Additionally, the lubrication between surfaces has a crucial effect on frictional behavior, because it reduces both the adhesion and hysteresis components of friction. The smoothened surfaces possess reduced viscoelastic deformation from surface asperities, which leads to lower friction levels [2].

Adhesion is generally recognized to consist of the creation and breaking of junctions at a molecular level (attach to counter surface, stretch, detach, relax, and re-attach), which occurs at asperity peaks, where the fluid film (if available) is extremely thin and has properties distinct from the bulk lubricant in the voids [2,12,13]. For the majority of polymers, the Van der Waals and hydrogen bonds are typical [11]. If the interfacial bonding is stronger than the cohesion of the weaker material, the material is fractured and wearing takes place. Otherwise, the fracture occurs at the interface [11]. During the rapid detachment and relaxation phases of the rubber molecules and their counterparts in each cycle, the elastic energy stored in the polymer chains is dissipated as heat, and this is assumed to be the origin of the adhesion component of friction [12,13]. The adhesion friction, which is expected to occur more on smooth elastomer surfaces [12,13] sliding over a hard surface, decreases with a decrease in Young's modulus and it is a function of the viscoelastic properties of the elastomer depending on the temperature and the sliding velocity [2].

A sliding elastomer can flow readily over the asperities of the counterpart and comply with their contours. This flowing action produces the deformation component of friction, which is called hysteresis [2]. The interface hysteresis occurs as a result of energy loss incorporated with the internal damping within the viscoelastic body (internal friction) [2,13]; however, the hysteresis increases with a decreasing Young's modulus [2].

Most oil and gas industry operations are in the presence of fluids, and the elastomeric seals, in static and dynamic applications, interact with liquids. Therefore, the determination of the tribological performance of elastomers both in contact with a solvent and under dry conditions is indispensable to understand the material's behavior [2,3,14]. The interaction of liquid with elastomers may result in an absorption process by the elastomer (swelling), which could change the chemical and physical material properties [9,15]. The chemical changes are expected to deteriorate irreversibly and still affect the properties after the solvent has fully dried out [15]. The monomers of the elastomer and their polarity determine the affinity for liquid absorption, where polar solvents are more compatible with polar substances and non-polar solvents are more compatible with non-polar substances and more likely to be dissolved [16–18]. The solubility parameter (δ), which is a thermodynamic property related to the energetic interaction between the liquid and the elastomer molecules, seems to explain mainly the liquid–elastomer interaction. When substances with the same or similar δ values are in

contact, they are likely to have an affinity for each other. Therefore, if the liquids have the same or closer δ values compared to the elastomer, the possibility to become absorbed into the elastomer increases and vice versa [15]. Additionally, the glass-transition temperature (T_g), crosslinking structure, amount of filler, working temperature, and specimen geometry influence this interaction [15,19]. In the equilibrium swelling state, the rubber–solvent interaction is maximized, whereas the rubber–rubber interaction decreases, leading to a total change in the conformation of polymer segments and chain entanglements [20]. Additionally, liquid intake into the material leads to a detachment process of the filler–rubber bonds, which are physically bonded [21], or even to a plasticizing effect [20,21]. Therefore, the properties are expected to be increasingly modified with the amount of swelling, which could be measured with the volume increase or the weight change after immersion.

There are very few published works dealing with the evaluation of the tribological performance after the swelling-induced ageing of elastomers. Mofidi et al. [2,22] tested the tribological behavior of elastomers aged in different oils (mineral, ester-based, and poly-alpha-olefin (PAO)) [2] and the influence of lubrication on abrasive wear [22]. They observed a higher COF reduction after ageing in ester-based synthetic oils compared with the mineral oils or PAOs for their nitrile butadiene rubber (NBR) used in the experiments [2], and in the lubricated conditions, they observed lower wear and a lower COF [22]. Although hydrogenated nitrile butadiene rubber (HNBR) is a widely used material in the oil and gas industry [1], some previous research efforts examining the effect of swelling-induced ageing on the tribology properties of HNBR are hard to find. However, there are some published works separately addressing the tribological properties of HNBR [23–27] and the influence of the swelling-induced ageing of HNBR on a change of the material's properties [16,19,28]. For example, Roche et al. [23] studied the influence of ageing on the tribological behavior of HNBR that was surface modified by ion implantation. They experienced greatly improved tribological properties by introducing a high-hardness coating layer to HNBR. Felhös et al. [24] experimented on the tribological properties of peroxide-cured HNBR with different multiwall carbon nanotube (MWCNT) and silica contents under dry sliding and rolling conditions against steel, and they observed that the filler amount has a progressive effect on the COF and wear resistance, while the MWCNT is a much better filler than silica. Similarly, Xu et al. [26] tested the friction and wear of HNBR with different fillers under dry rolling and sliding conditions and they experienced that the carbon black (CB)-containing and MWCNT-containing HNBR compounds possessed higher wear resistance compared with a silica-filled HNBR. Yuqin et al. [27] researched on the impact, friction, and wear properties of HNBR composites filled with silane-treated silicon carbide (SiC) and graphite. They experienced that the friction and wear behavior of the filled composites improved mostly when graphite-treated and silane-treated SiC were added together due to the synergistic effect between them. Karger-Kocsis et al. [25] conducted tests identifying the mechanical and tribological properties of rubber blends composed of HNBR and in-situ produced polyurethane and they found that the resistance to wear increased with Polyurethane (PU) hybridization into HNBR.

Therefore, the objective of this scientific work is to identify the effect of the combined action of swelling-induced ageing and tribological properties of HNBR in swollen and de-swollen conditions. This helps in improving its wear resistance and extending its service life under various conditions related to oil and gas field applications. Furthermore, the scientific paper focuses on the investigation and correlation between mechanical properties and surface properties in different environments. A clear understanding of the failure mechanism provides better insight to predict the service life of rubber products.

2. Experiments

2.1. Materials

An HNBR model material, which has 36% acrylonitrile (ACN) content, is peroxide cross-linked, and is filled with carbon black (85 phr) and plasticizers in a common amount, was selected for these

investigations. The manufactured compound was provided as disk plates and as specially designed disk specimens.

2.2. Specimens and Experimental Methods

In order to investigate the tensile properties of HNBR in different swelling conditions, un-swollen (no contact with solvent), swollen (immersed in a solvent until the equilibrium state), and de-swollen (swollen and then dried to remove the solvent out of the material) samples were tested. The swelling tests were conducted by exposing HNBR to standard solvents according to ASTM D471-06, i.e., IRM 903 at 100 °C and an iso-octane/toluene mixture (70:30, vol %) at 70 °C for 168 h [16]. To obtain the de-swollen state, the samples which were swollen in IRM 903 were placed in a vacuum oven at 50 °C for 4 h, and the samples which were swollen in the iso-octane/toluene mixture were placed in an air-circulating oven at 50 °C for 26 h. The drying time was determined by repeatedly measuring the weight of the specimens until the equilibrium state was reached. The other swollen specimens were rushed to sample preparation and testing. For each condition, five tensile test specimens were used to ensure reproducibility. Besides the mechanical performance, the swelling amount and density were measured in different swelling test setups. A balance and density kit (XS205DU, Mettler Toledo, Greifensee, Switzerland) measured the weight (in air to the nearest 1 mg) and the density (by the buoyancy method). The mean value and standard deviation of the results were calculated from these measurements and used for analysis.

The surface properties of HNBR in the un-swollen, swollen, and de-swollen states were investigated through tribological measurements. The swollen (in IRM 903 or in the iso-octane/toluene mixture) and de-swollen conditions were achieved with similar steps as explained above. The weight before swelling, after swelling, and after the tribological tests was measured to the nearest 1 mg.

The worn surface morphologies were analyzed by scanning electron microscopy (SEM) to obtain a better understanding of the friction and wear behavior and special damage mechanisms at every test stage. The specimen surfaces were analyzed with FTIR in ATR mode to identify the possible chemical and structural changes due to swelling-induced ageing.

In the following sections, the specimen dimensions and test parameters are summarized.

2.2.1. Tensile Tests

Smooth dumbbell specimens (S2) (DIN 53504) were punched out from plates (in un-swollen, swollen, and de-swollen conditions) just before the tensile tests. These specimens possess a thickness of ~2 mm and a width of 4 mm. All of the tests were performed with a Zwick universal testing machine (Zwick Roell, Test expert, Ulm, Germany) with a 1 kN load cell at a constant crosshead speed of 200 mm/min and a gauge length of 25 mm according to DIN 53504.

2.2.2. Tribological Tests

All tests were conducted in a rotational Tribometer TE93 (Phoenix Tribology Ltd., Newbury, UK) under a 50 N load at 118 rpm speed for 168 h. The specially designed disk specimen (with inner and outer diameters of 21 mm and 62 mm, respectively) contains a homogeneous lip geometry for the investigation of the friction behavior in line contact with the counter surface. The test parameters and the specimens were improved by previous research work [29]. The specimen's front view and a sketch of the cross-section and lip geometry are shown in Figure 1a,b, respectively. The specimen was mounted onto the rotational drive of the machine, whereas the counterpart was in the static state. The counterpart is a hollow cylindrical steel disk with 54 mm and 38 mm outer and inner diameters, respectively; the average surface roughness (R_a) was measured utilizing a non-contact Profilometer (Microprof, FRT GmbH, Bergisch Gladbach, Germany). The surfaces of the counterpart were polished using a grinding pass, giving them nearly identical surface roughness structures, R_a ~0.03 µm. Every test was conducted with similar amounts of Vitrea 68 (~80 mg) in liquid form as

the lubricant between the counterpart and the specimen. The tested samples were carefully washed with diluted iso-propanol before measuring the sample weight and before surface observations.

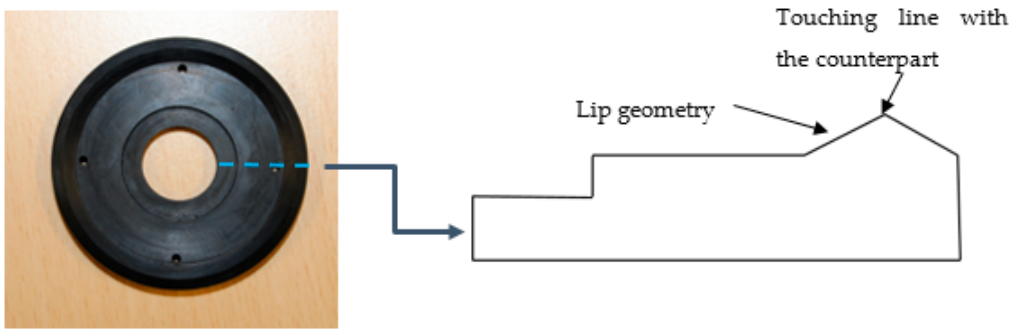

Figure 1. The tribology specimen: (**a**) the front view and (**b**) a sketch of the radial cross-section of the specimen.

2.2.3. Surface Observation

The surface topography of every fresh specimen was investigated to maintain the accuracy of the contact surfaces and lip geometry by optical microscope (Alicona Infinite Focus, Graz, Austria). The wear surfaces of the tribo-tested samples were inspected by utilizing SEM (Tescan VEGA-II, Brno, Czech Republic) and a light microscope.

2.2.4. Fourier Transmission Infra-Red (FTIR) Spectrometer Test

The surface layer of the lip geometry of tribo-tested samples was analyzed with FT-IR spectroscopy in ATR mode using a Spectrum GX 75611/2 (Perkin Elmer, Liantriasant, UK) in the spectra range of 600–4000 cm^{-1}.

3. Results and Discussion

In the following section, the swelling behavior, the bulk property changes of the swollen samples, and the swelling-induced ageing effects on tribological properties are compared. The possible microstructural changes and the chemistry involved in the interaction with the solvents, which affect the bulk properties, surface properties, and SEM-assisted surface analysis, are discussed as well.

The influences of the swelling-induced ageing on the tensile properties of HNBR are shown in Figures 2 and 3 for the samples immersed in iso-octane/toluene and IRM 903, respectively. The tensile strength (σ_R), the elongation at break (ε_R), and the stress at 50% strain ($\sigma_{50\%}$) are compared in Figure 2a. As depicted, the σ_R values are drastically decreased in the swollen state compared with the un-swollen, up to 60%; however, after de-swelling, the σ_R values are fully restored. A similar behavior was observed for ε_R, where the swollen values show a reduction from the un-swollen values (up to ~74%), and after de-swelling they are recovered or even higher compared with the un-swollen properties. Due to swelling, the $\sigma_{50\%}$ is also reduced by up to half of its un-swollen values, ending up in a fully recovered state after de-swelling or with even slightly higher values. The swelling amount (density and weight) changes, as well as the stress-strain behavior, are shown in Figure 2b,c, respectively, for the samples which were immersed in iso-octane/toluene. In the swollen state, the sample weight is increased by up to ~15%, and after de-swelling, a slight weight loss is recorded and the density is changed accordingly (the volume change in the swollen condition (~30%) is more significant compared to the change of the weight). By contrast, as Figure 3a summarizes, for samples immersed in IRM 903, the σ_R, ε_R, and $\sigma_{50\%}$ of the HNBR did not deteriorate much; they also did not deteriorate much in the de-swollen state. As shown in Figure 3b,c, swelling increases the weight slightly (~5.6%), and this effect mostly persists (~4.9%) in the material even after the evaporation and no significant density change

was recorded. As the other mechanical properties proved, the stress-strain behavior (Figure 3c) is not changed significantly in samples in contact with IRM 903. The equilibrium swelling was reached after 24 h of immersion time, and the volume increase was recorded as 27% and 9% in the iso-octane/toluene mixture and the IRM 903, respectively.

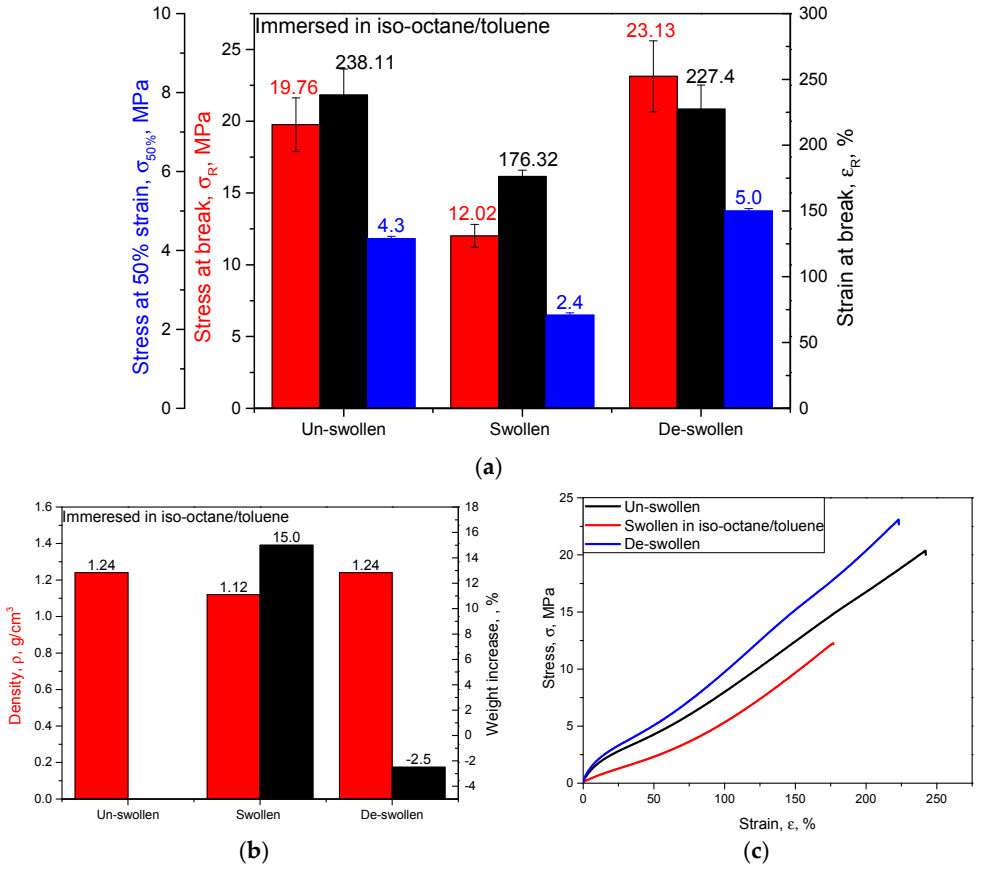

Figure 2. Influence of swelling of hydrogenated nitrile butadiene rubber (HNBR) in iso-octane/toluene at 70 °C for 168 h and after de-swelling compared with un-swollen samples: (**a**) strength at break, strain at break, and stress at 50% strain; (**b**) density and weight increase in percent; (**c**) stress-strain behavior.

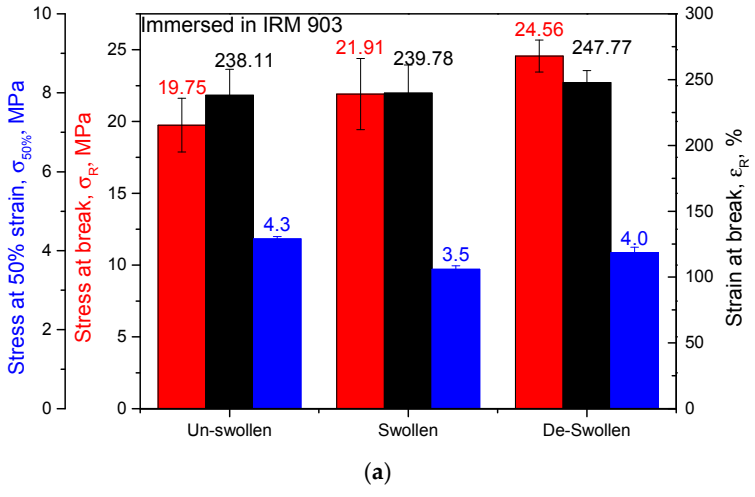

Figure 3. *Cont.*

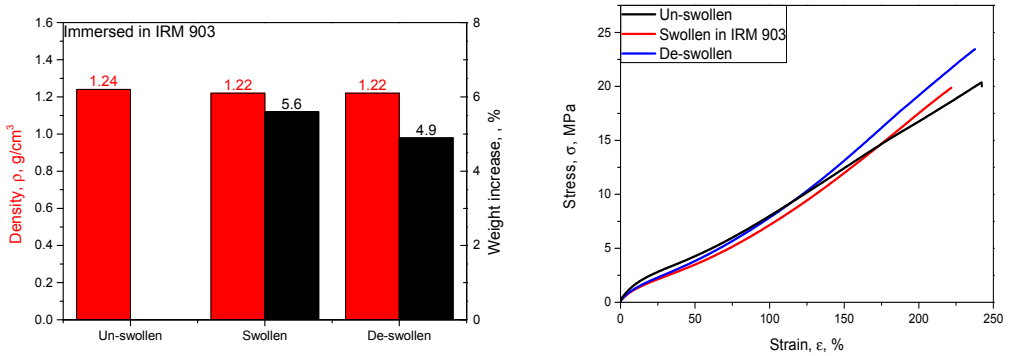

Figure 3. Influence of swelling of HNBR in IRM 903 at 100 °C for 168 h and after de-swelling compared with un-swollen samples: (**a**) strength at break, strain at break, and stress at 50% strain; (**b**) density and weight increase in percent; (**c**) stress-strain behavior.

Swelling is mainly responsible for the intra-molecular motions of segments and rearranging the long molecular chains, including the shifting of chain entanglements, elastomer-filler de-bonding, and even plasticizing [16,20,21]. Therefore, the observed results in the swollen states, the degraded strength at break, and the decreased stiffness could be attributed to released entanglements, the elastomer-filler de-bonding mechanism, and plasticizing. The elastomers possess free volume within the molecules, which gives molecules the freedom to rearrange during external loading. However, in the swollen state, the presence of solvents in the material stretches the molecules and that results in reduced strain at break or decreased ductility in the swollen state. Nevertheless, the physically impaired tensile properties are fully restored in the de-swollen states of those samples that were swollen in iso-octane/toluene due to re-arranging entanglements, possible elastomer-filler bonding, and regained free volume within the molecules in fully dried-out conditions. The HNBR seems more compatible to the contact with the iso-octane/toluene mixture compared with IRM 903, which are equivalent to gasoline or diesel fuels and petroleum, respectively. Solubility parameters (δ) for the toluene and iso-octane were identified in the literature as 8.97 and 6.9 $(cal/cm^3)^{1/2}$, respectively, and meanwhile, the IRM 903 and HNBR have δ as 16.9 $(cal/cm^3)^{1/2}$ and 9.7 $(cal/cm^3)^{1/2}$, respectively [30]. Therefore, iso-octane and toluene as aromatic, low viscosity, volatile solvents, which possess closer solubility parameters to HNBR, exhibit a greater swelling effect in contact with the HNBR samples [31]. However, the HNBR swells only slightly in IRM 903 due to the low compatibility between the solubility parameters based on a polarity mismatch and higher viscosity. Greater swelling correlates with the degree of tensile properties' reduction in swollen conditions in these two solvents. Additionally, the butadiene part of HNBR and the higher viscosity of IRM 903 create difficulties in removing IRM 903 from the sample by conventional drying methods to obtain the de-swollen condition [1,31]. Therefore, IRM 903 would not be ideal for finding the de-swelling effect on mechanical properties, but it is suitable to analyze the effects of swelling.

A typical test result from the TE 93 test machine is shown in Figure 4, which displays the friction coefficient, the temperature on the specimen surface and on the counterpart, and wear in terms of dimensional change with test time. The results show that the COF and the specimen surface and counterpart temperatures are stabilized after a running-in time.

The surface properties of the tested HNBR specimens in different swollen conditions (un-swollen, swollen in IRM 903, swollen in IRM 903 and de-swollen, swollen in iso-octane/toluene and de-swollen) are summarized in Figure 5, comparing: (a) the wear (mass and dimensional) losses, (b) the friction coefficients (COFs), as well as (c) the specimen surface temperature. The tribological properties after swelling in the iso-octane/toluene mixture were not tested due to the highly volatile nature of that solvent, but the samples immersed in IRM 903 were tested in both swollen and de-swollen conditions.

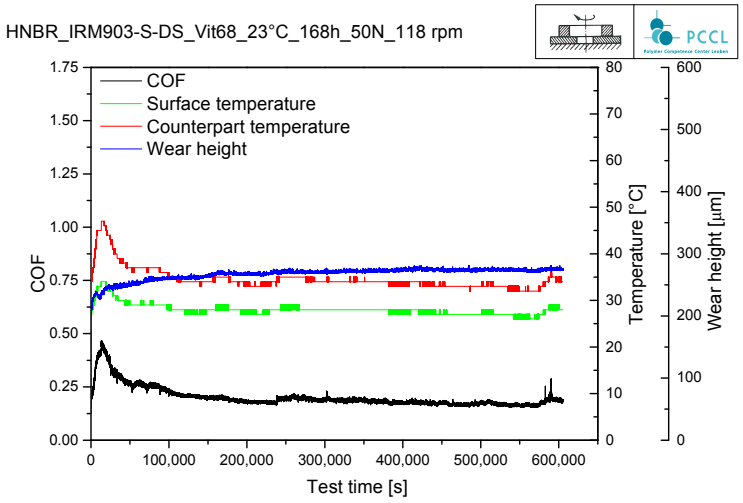

Figure 4. A typical surface analysis test result from TE 93: a result of sample swollen in IRM 903, which shows COF, specimen surface temperature, counterpart temperature and wear in terms of dimensional change with testing time.

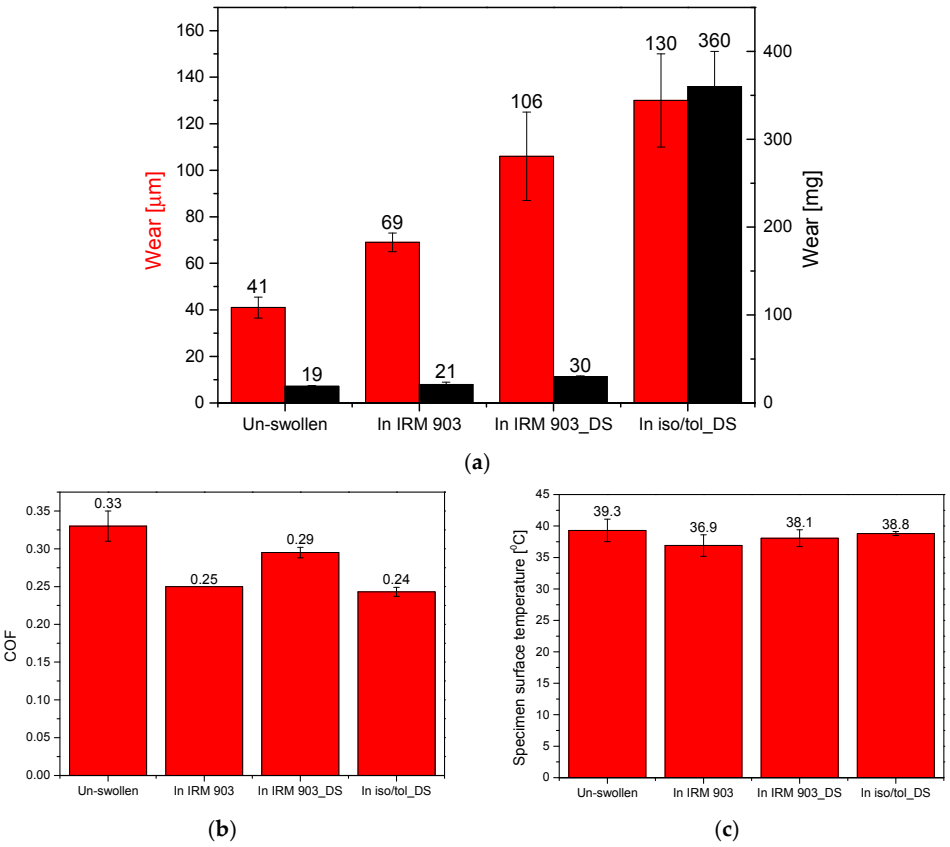

Figure 5. Tribological property changes of HNBR in different conditions; un-swollen, swollen in IRM 903 at 100 °C for 168 h and after de-swelling, swollen in iso-octane/toluene at 70 °C for 168 h and subsequently de-swollen: (**a**) Wear losses (weight and dimensional); (**b**) COF; and (**c**) specimen surface temperature.

As depicted in Figure 5, the un-swollen samples demonstrate the lowest wear losses in dimensions and weight, but the highest friction coefficient and the highest specimen surface temperature compared with the other tested conditions. The samples, which were swollen in IRM 903, show a relatively

higher wear, lower COF, and lower specimen surface temperature compared with the un-swollen condition; in the de-swollen state, the wear is even greater than that in the swollen state; however, the COF and the specimen surface temperatures are in between those of the swollen and un-swollen results. Nevertheless, the highest wear loss was recorded for the samples in de-swollen conditions after swelling in iso-octane/toluene, irrespective of the lowest COF. As shown in Figure 5a, the greatest magnitude of wear losses, in weight and dimensions, was recorded in the swollen and de-swollen conditions compared with the un-swollen state. For example, the weight losses of samples swollen in IRM 903 and those of the de-swollen samples that had previously been immersed in IRM 903 and in iso-octane/toluene are 1.1, 6, and 18 times greater, respectively, compared with the weight loss of the un-swollen sample. Evidently, the extent of material removal in the de-swollen samples immersed in iso-octane/toluene was remarkably higher as compared to the other conditions.

In between the samples and counterparts, a similar amount of Vitrea 68 was used for lubrication in every tribology test, maintaining the same condition for every test. This high viscosity-index mineral oil was specially chosen due to its ability to provide superior lubrication and its good compatibility with HNBR, where minimal swell, hardness, and change of oil viscosity over the temperature range are expected in service [32]. Therefore, a minimum effect from the lubricant on the chemical changes of the material and among different tests are expected. The specimens were gently cleaned with diluted iso-propanol after the tribology measurements, as it is widely used as a cleaning agent due to its ability to dissolve mineral oils and its highly volatile nature. Therefore, only the removal of the lubricant on the surface, and no effect on the final weight measurements, is expected. After washing, the specimens were dried again in an air-circulated oven at 50 °C until the weight was constant, implying that no residuals of oil or of the iso-propanol itself should be left on the sample surfaces. Thereafter, the weight measurements and surface analysis of the tested samples were conducted.

In order to understand the mechanisms of wear involved in testing different conditions, the specimen surfaces were examined by scanning electron microscope. The surface texture of the un-swollen samples before testing and after testing are compared in Figure 6a,b, respectively. The surface morphologies of the worn tracks of samples immersed in IRM 903, in IRM 903 then de-swollen, and in iso-octane/toluene then de-swollen are displayed in Figures 7–9, respectively. The surface texture of the un-swollen samples after the sliding test (Figure 6b) seems worn off (some small particles) compared with the sample before testing (Figure 6a); however, in general, it still looks smooth and dense.

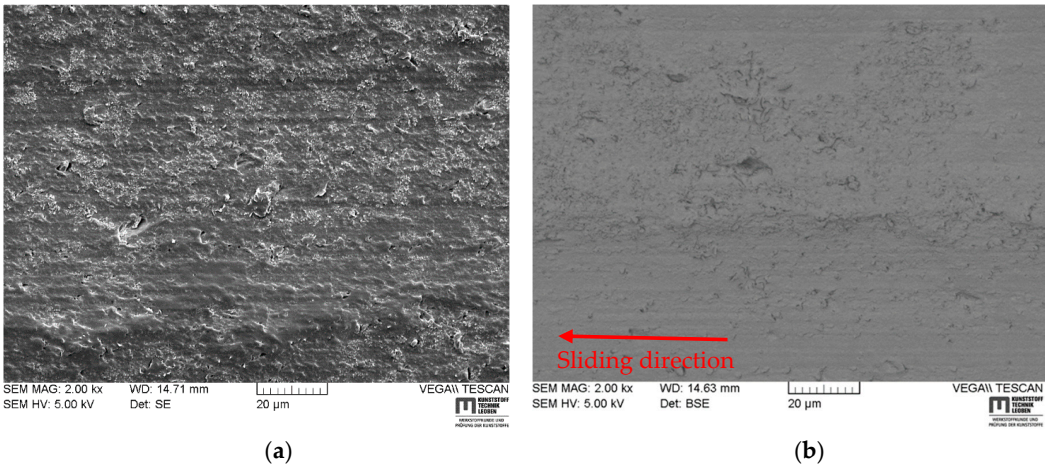

(**a**) (**b**)

Figure 6. Typical SEM images of HNBR un-swollen samples: (**a**) before the tribo-test; (**b**) after the tribo-test.

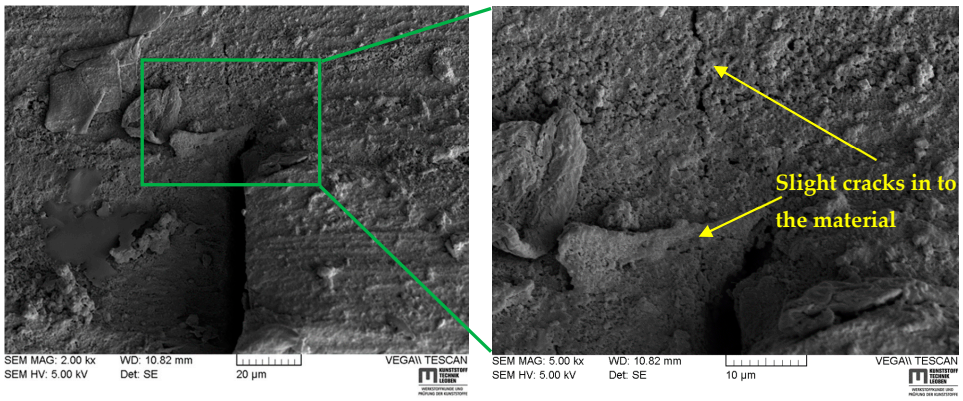

(**a**) (**b**)

Figure 7. Typical SEM images after the tribo-tests of samples immersed in IRM 903: (**a**) tearing cracks perpendicular to the sliding direction and removal of small particles; (**b**) magnified area around the vicinity of a crack.

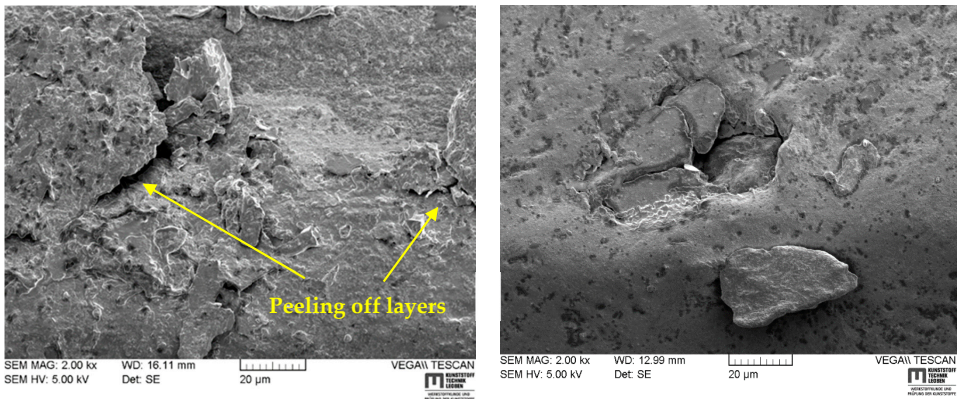

(**a**) (**b**)

Figure 8. Typical SEM images after the tribo-tests of samples immersed in IRM 903 and de-swollen: (**a**) wear behavior in a manner of the peeling off of layers; (**b**) wear behavior in a manner of removing bigger particles from the surface.

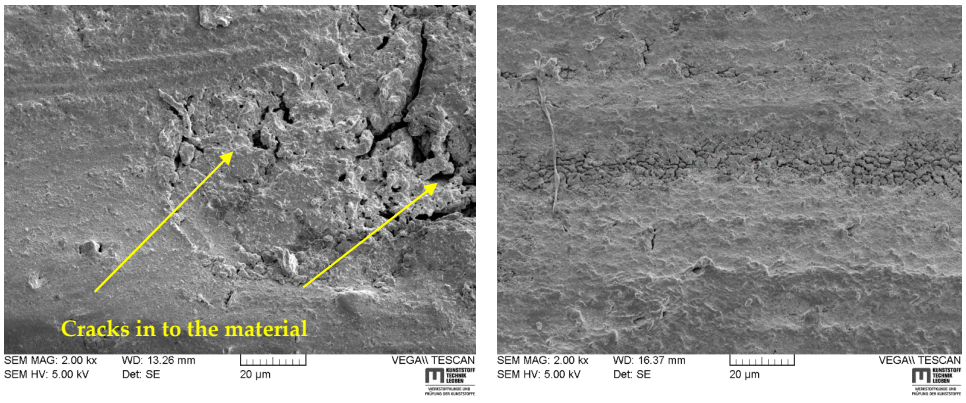

(**a**) (**b**)

Figure 9. Typical SEM images after the tribo-tests of samples immersed in iso-octane/toluene and de-swollen: (**a**) a large wear surface with pitting morphology and cracks into the material; (**b**) deep worn tracks and cracks into the material.

The swollen samples in IRM 903 exhibit ruptures perpendicular to the sliding direction, including relatively larger debris, as shown in Figure 7a and in the magnified view (Figure 7b), where slight cracks around the rupture and uneven surface roughness can be seen. Lamellar structures, originating from the peeling of surface layers, were apparent on the worn surface of samples swollen in IRM 903 and subsequently de-swollen, as visible in Figure 8a. Additionally, some larger spallings were observed as shown in Figure 8b. Larger worn-off surfaces with pits and a greater density of defects penetrating into the material were evident in samples swollen in iso-octane/toluene and subsequently de-swollen (Figure 9a). Further, the surface contains worn-off tracks with a larger number of cracks as shown in Figure 9b.

With respect to the observed results, the surface properties and the surface analysis through the SEM images are in good agreement. The absorbed solvent could emerge to the surface with the applied force and act as an additional lubricant between the sample and the counterpart; this could explain the relatively lower COF measured with the IRM 903 swollen samples compared with the samples in an un-swollen condition. An additional test series where IRM 903 was used as a lubricant, instead of Vitrea 68, revealed a higher COF compared with Vitrea 68 used in the same amount as a lubricant. For example, the un-swollen HNBR with IRM 903 (naphthenic base oil) as lubricant showed a COF of 0.41 instead of a value of 0.33 with Vitrea 68 (paraffinic base oil). Mofidi et al. [2] observed a similar trend with their tests comparing the COF of NBR in the presence of different base fluids. IRM 903 has a middle range of viscosity compared with Vitrea 68, which has high viscosity (the kinematic viscosities of Vitrea 68 and IRM 903 are 68 mm^2/s and 32 mm^2/s, respectively, at 40 °C) [2,32,33]. However, Mofidi et al. [2] did not find any correlations between the viscosity of the lubricant and the COF. Therefore, IRM 903 is in fact a lubricant, though less effective than Vitrea 68, and its release from a swollen sample can contribute towards further reduction in friction compared to the un-swollen or de-swollen samples as witnessed in Figure 5b. However, the chemical reactions between those highly viscous, anti-oxidative paraffinic and naphthenic base oils [32,33] were not considered in this study, which was expecting a minimal effect. The increased wear in terms of weight and dimension loss in the swollen condition could be attributed to the decrease in the shearing strength of the rubber surface as a result of the weak properties of swollen rubbers [34]. The observed larger tearings/ruptures could also confirm this behavior (Figure 7). The swelling of rubber alters the molecular network with disentanglements, the de-bonding of physical bonds, and even a plasticizing effect [16,20,21]. Additionally, in swollen states, decreased density values were observed as a result of the liquid's penetration, including a slightly porous morphology on the surface, as shown in Figure 7b. These phenomena indicate the lower wear resistance and the relatively larger debris on the surface of samples in a swollen condition compared with those in an un-swollen condition. A lower specimen temperature is expected in swollen samples with respect to the lower COF, lower energy dissipation, and better thermal conductivity with some additional oil in the material [2,35]. Under the test conditions, the samples swollen in IRM 903 were not fully de-swollen; however, a surface dryness was expected. Therefore, the COF and the surface temperature of de-swollen samples could be anticipated to be intermediate between those of swollen and un-swollen samples. However, a higher wear loss was recorded compared with both samples in the swollen state and samples in the un-swollen state. This tendency was revealed in the SEM images with worn-off layers and relatively bigger worn-off particles as shown in Figure 8. In the swollen conditions, the specimen surface was offered some lubrication by absorbed solvent as a viscous protective film and this could alleviate the local concentrations of tearing force, which could presumably be responsible for the detachment of particles [7]. The samples in a de-swollen state after being swollen in iso-octane/toluene showed the highest wear; for instance, wear is ~18 times and 12 times greater compared with the un-swollen samples and the samples in de-swollen conditions after being swollen in IRM 903, respectively, while showing the lowest COF in the present test conditions. The SEM-assisted analysis also revealed deep and larger pits on the contact surface, with densified cracks into the material on worn-off surfaces (Figure 9). Iso-octane and toluene, being low molecular weight and highly volatile aromatic solvents, swell HNBR to a relatively higher degree (~30% in

volume and 15% in weight) compared to IRM 903, a highly viscous, non-volatile mineral oil (~9% in volume and 5.7% in weight), as shown in Figures 2 and 3. Therefore, the larger swelling seemingly adversely affected the wear resistance of the HNBR while lowering the COF.

Therefore, an additional FTIR-ATR analysis was conducted to gain knowledge about any chemical structural changes introduced to the materials' surfaces as a result of swelling-induced ageing which remained even after the de-swelling. Figure 10 illustrates the typical IR spectra of HNBR after the tribo-tests in different swelling-induced ageing conditions (de-swollen state after being swollen in IRM 903 and iso-octane/toluene) compared with the un-swollen state. As depicted, every condition shows HNBR signature peaks, i.e., the peaks in the range of 2800–3000 cm^{-1} corresponding to C–H stretching vibrations, the peak at 2238 cm^{-1} for –CN, and the peak at 1433 cm^{-1} for $–CH_2$ groups. Additionally, the peaks at 1733, 1169, and 1108 cm^{-1} were apparent in the un-swollen samples, which could be attributed to the C=O stretching vibration, the C–O–C stretching vibration, and the $–CH_3$ group, respectively. This could reveal the presence of additives in the used HNBR, i.e., stearic acids, acyl esters, aliphatic acids, rubber anti-oxidants (TMQ), and curing agents [36–39]. The peaks corresponding to additives were seemingly reduced to some extent in the de-swollen states compared with the un-swollen states. The peaks in the range of 2800–3000 cm^{-1} were also reduced, which could also be attributed to some level of paraffin (a typical processing agent used in rubber) [37,38] in the material and a reduction in de-swollen conditions. Therefore, it seems that the solvents extracted the soluble additives, which is a physiochemical process [38], from the material, and this could be also seen from the weight loss (Figure 2b) or hardened bulk properties in samples in a de-swollen condition (Figures 2c and 3c). However, additive extraction is seemingly adversely affecting the surface properties, because the additive breakdown from the material matrix creates a non-uniform density distribution and a porous nature on the surface [36]. The SEM-based surface observation proved a similar behavior (Figures 7–9). Therefore, higher swelling causes a higher surface degradation/softness and this condition persists even in de-swollen conditions. Similar behavior was observed in the literature for fluoro-elastomers with swelling-induced ageing [34].

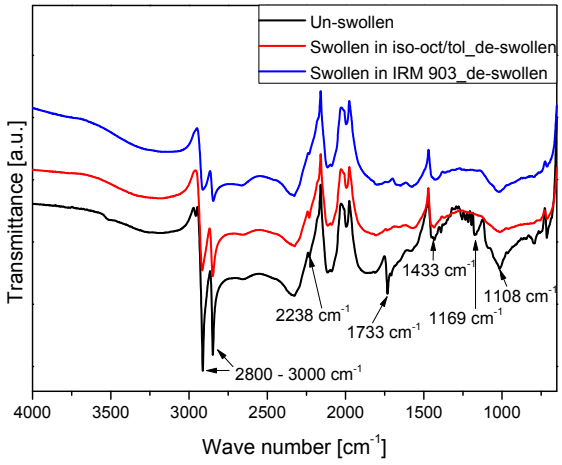

Figure 10. The FTIR spectra in ATR mode of the tribo-tested samples in different conditions.

The friction and wear properties of the HNBR that was used are rather complex, because the specimen in the test setup rotates continuously and stress and strain apply in the normal and the tangential directions on the counter surface. Owing to the curved and entangled nature of rubber molecules, they can withstand considerable lateral deformations without fracture by the stretching and twisting of chains [4,8]. Wear is generally based on tearing or smearing: small particle removal from the surface by frictional forces (smearing) and subsequent removal of larger particles by tearing. When the shear stress surpasses the cohesive strength of the polymer chains, a fracture initiates by the propagation of the crack along the root of the contact area [8,10]. If crack initiation is more

difficult to achieve, the whole wearing process is retarded. Thus, overall wear is dependent upon crack initiation [10].

Under the present test conditions, sliding occurred on a relatively smooth surface, so friction was expected through the stick-slip mechanism (adhesion). During adhesion, at the interface, the shear stress increases continuously with time and the crack grows when the local shear stress reaches the critical value [12]. The damage mechanisms of the un-swollen sample surface (Figure 6b) correlate with the smearing wear mechanisms, where small particles were worn off due to a relatively hard counterpart surface without any swelling-induced ageing. The swollen samples in IRM 903 showed a relatively aged surface with some tiny pores on the surface and some relatively larger worn off particles. Friction due to adhesion is retarded to some extent with IRM 903 on the surface in the swollen condition. In both de-swollen states, the samples show higher wear, forming lamellar spallings and a pit-like surface with particles rolling off. Therefore, this damage mechanism could be explained as shown in Figure 11.

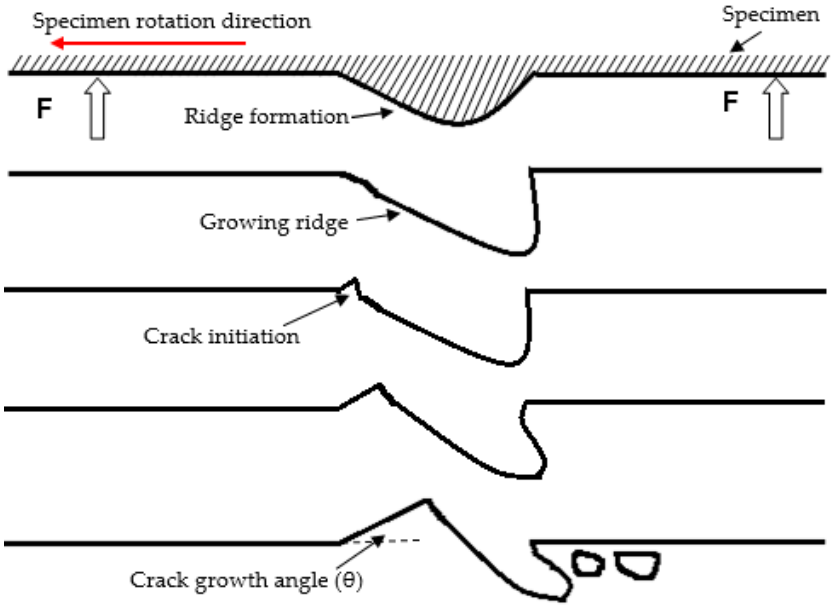

Figure 11. Schematic illustration of the possible mechanism of the wearing off of particles in rubber sliding against a solid counterpart. Stages of ridge formation and crack growth on the specimen's surface when stresses exceed the weakened polymer chain strength. Specimen rotation direction and force (F) direction on the surface from the counterpart are as illustrated.

When the stress is transferred to a softer surface, for instance, due to the swelling effect, the lower modulus of the material can increase the normal deformation, which could increase the contact area and the shear effect on the material, intensifying the wear degradation [4]. Additionally, as shown in Figure 11, the repeated deformation accumulates in the surface layers into a roll formation, i.e., ridges. The swelling of HNBR, especially in iso-octane/toluene, results in cracks and voids on the surface (Figure 9). As the FTIR spectra revealed (Figure 10), some additives are extracted from the surface, creating small voids in the elastomer and acting as a possible initiator of internal failure as a result of unbounded elastic expansion [9]. Based on the density of the surface defects, the thickness of ridges is attenuated or increased; severely impaired surfaces initiate the cracks at larger angles (θ) and drive the crack deeper into the material as illustrated in Figure 11. Additionally, Lv et al. [34] observed a reduction of cross-link density and an increase in the proportion of tail suspension chain (%) in their NBR material with the degree of swelling. The swelling-induced ageing lead to surface softness through voids and molecular structure destruction and it drives chain elongation and even

easy chain breakage [9]. Therefore, the worn surface further shows the formation of grooves and the removal of material as chunks (bigger particles).

4. Summary and Conclusions

In the present work, an HNBR model material was used to identify the tribological and mechanical behavior under certain swollen conditions. A greater degree of swelling of the HNBR in an iso-octane/toluene (70:30, vol %) mixture was experienced compared with a relatively lower effect in IRM 903. Weaker mechanical properties were observed in the presence of solvent in the material, and the degradation magnitude was correlated with the degree of swelling; in fully de-swollen states, the un-swollen properties were regained. In swollen states, the material surface properties were impaired with a lower friction coefficient and higher wear loss, and in de-swollen conditions, the wear loss magnitude was even greater. The presence of the solvent increased the wear loss, and the degree of swelling correlated with the surface property degradation, where higher mechanical property degradation was experienced with the degree of swelling. However, an even higher degree of wear was experienced in de-swollen conditions due to the permanently altered surface as a result of swelling, but the absence of solvent releasing from the material in the de-swollen condition could add further lubrication to the surface. In un-swollen conditions, wear through smearing was witnessed, but in swollen and de-swollen conditions, bigger particles were worn off through tearing. Surface defects due to swelling-induced ageing could more easily initiate cracks on the ridges, which accumulated as a result of constant sliding, and the degree of swelling could determine the intensity of the soft surface, which would help the crack to grow deeper in to the material. Under the tested conditions, in the de-swollen states, the bulk mechanical properties were almost recovered, in contrast to the surface properties, which were greatly impaired. The present study could be improved by adding deeper investigations of the effects of swelling-induced ageing from different solvents in different conditions and considering effects with lubricant at different temperatures. Furthermore, tribological properties with a simulation method for predicting the service life of lip seals will be implemented in a future work.

Acknowledgments: The research work was performed at the Polymer Competence Center Leoben GmbH (PCCL, Austria) within the framework of the COMET-program of the Federal Ministry for Transport, Innovation, and Technology and the Federal Ministry of Economy, Family, and Youth with contributions from the material science and testing of polymers of the Montanuniversität Leoben and SKF Sealing Solutions Austria GmbH. The PCCL is funded by the Austrian Government and the State Governments of Styria, Lower Austria, and Upper Austria.

Author Contributions: Andreas Hausberger developed the tribology test setup and the test procedure, including the specimen geometry; Winoj Balasooriya conducted the tests and Chao Wang helped implement the tribology test procedure; Winoj Balasooriya, Bernd Schrittesser, Chao Wang, and Andreas Hausberger analyzed the data and discussed the results; Thomas Schwarz contributed the materials and specially designed specimens; Gerald Pinter consulted on the research work and held scientific discussions; Winoj Balasooriya conducted the literature research and wrote the paper.

Conflicts of Interest: The authors declare no conflicts of interest.

References

1. Hofmann, W. *Rubber Technology Handbook*, 2nd ed.; Hanser: Munich, Germany; Vienna, Austria; New York, NY, USA, 1989.
2. Mofidi, M.; Kassfeldt, E.; Prakash, B. Tribological behavior of an elastomer aged in different oil. *Tribol. Int.* **2008**, *41*, 860–866. [CrossRef]
3. Chandrasekaran, M.; Batchelor, A.W. In situ observation of sliding wear tests of butyl rubber in the presence of lubricants in an X-ray micro focus instrument. *Wear* **1997**, *211*, 35–43. [CrossRef]
4. Tayeb, N.S.M.E.; Nasir, R.M. Effect of soft carbon black on tribology of de-proteinised and polyisoprene rubbers. *Wear* **2007**, *262*, 350–361. [CrossRef]
5. Wang, L.L.; Zhang, L.Q.; Tian, M. Mechanical and tribological properties of acrylonitrile butadiene rubber filled with graphite and carbon black. *Mater. Des.* **2012**, *39*, 450–457. [CrossRef]

6. Gent, A.N.; Pulford, C.T.R. Mechanisms of rubber abrasion. *Appl. Polym. Sci.* **1983**, *28*, 943–960. [CrossRef]
7. Smith, G.C.; Park, D.; Titchener, K.J.; Davies, R.E.; West, R.H. Surface studies of oil-seal degradation. *Appl. Surf. Sci.* **1995**, *90*, 357–371. [CrossRef]
8. Myshkin, N.K.; Petrokovets, M.I.; Kovalev, A.V. Tribology of polymers: Adhesion, friction, wear, and mass-transfer. *Tribol. Int.* **2005**, *38*, 910–921. [CrossRef]
9. Guo, F.; Jia, X.; Lv, M.; Wang, L.; Salant, R.F.; Wang, Y. The effect of aging in oil on the performance of a radial lip seal. *Tribol. Int.* **2014**, *78*, 187–194. [CrossRef]
10. Pandey, K.N.; Setua, D.K.; Mathur, G.N. Material behavior Fracture topography of rubber surfaces: An SEM study. *Polym. Test.* **2003**, *22*, 353–359. [CrossRef]
11. Gent, A.N. A hypothetical mechanism for rubber abrasion. *Coll. Polym. Sci. Polym. Eng. Univ. Akron* **1988**, *62*, 750–756. [CrossRef]
12. Persson, B.N.J.; Volokitin, A.I. Rubber friction on smooth surfaces. *Eur. Phys. J.* **2006**, *21*, 69–80. [CrossRef] [PubMed]
13. Persson, B.N.J. On the theory of rubber friction. *Surf. Sci.* **1998**, *401*, 445–454. [CrossRef]
14. Muller, H.K. *Fluid Sealing Technology: Principles and Applications*; CRC Press: New York, NY, USA, 1998.
15. Campion, R.P.; Thomson, B.; Harris, J.A. *Elastomers for Fluid Containment in Offshore Oil and Gas Production: Guidelines and Review*; Health and Safety Executive: Liverpool, UK, 2005.
16. Balasooriya, W.; Schrittesser, B.; Pinter, G.; Schwarz, T. Influence of HNBR ageing in oil field applications. *Rubber Fiber Plast. Int.* **2017**, *4*, 250–257.
17. Rinnbauer, M. *Technical Elastomers, the Basis of High-Tech Sealing and Vibration Control Technology Solutions*; SV Corporate Media GmbH: Munich, Germany, 2007.
18. Zhang, H.; Cloud, A. *Research Progress in Calenderable Fluoro-Silicone with Excellent Fuel Resistance*; Arlon Silicone Technologies Division: Bear, DE, USA, 2007.
19. Vidović, E. Development of lubricating oils and their influence on the seals. *Goriva I Maziva* **2014**, *53*, 220–235.
20. George, S.C.; knörgenb, M.; Thomas, S. Effect of nature and extent of crosslinking on swelling and mechanical behavior of styrene-butadiene rubber membranes. *Membr. Sci.* **1999**, *163*, 1–17. [CrossRef]
21. Diani, J.; Fayolle, B.; Gilormini, P. A review on the Mullins effect. *Eur. Polym. J.* **2009**, *45*, 601–612. [CrossRef]
22. Mofidi, M.; Prakash, B. The influence of lubrication on two-body abrasive wear of sealing elastomers under reciprocating sliding conditions. *Elastom. Plast.* **2010**, *43*, 19–31. [CrossRef]
23. Roche, N.; Heuillet, P.; Janin, C.; Jacquot, P. Mechanical and tribological behavior of HNBR modified by ion implantation, influence of aging. *Surf. Coat. Technol.* **2008**, *209*, 58–63. [CrossRef]
24. Felhös, D.; Karger-Kocsis, J.; Xu, D. Tribological testing of peroxide cured HNBR with different MWCNT and silica contents under dry sliding and rolling conditions against steel. *Appl. Polym. Sci.* **2008**, *108*, 2840–2851. [CrossRef]
25. Karger-Kocsis, J.; Felhös, D.; Xu, D. Mechanical and tribological properties of rubber blends composed of HNBR and in situ produced polyurethane. *Wear* **2010**, *268*, 464–472. [CrossRef]
26. Xu, D.; Karger-Kocsis, J.; Schlarb, A.K. Friction and wear of HNBR with different fillers under dry rolling and sliding conditions. *Express Polym. Lett.* **2009**, *3*, 126–136. [CrossRef]
27. Yuqin, T.; Wang, X.; Chi, Y.; Liu, H.; Zhou, T. Research on the impact and friction and wear properties of acrylonitrile butadiene rubber composites filled with SiC and graphite. *J. Thermoplast. Compos. Mater.* **2014**, *27*, 1013–1021.
28. Trakarnpruk, W.; Porntangjitlikit, S. Palm oil biodiesel synthesized with potassium loaded calcined hydrotalcite and effect of biodiesel blend on elastomer properties. *Renew. Energy* **2008**, *33*, 1558–1563. [CrossRef]
29. Hausberger, A.; Godor, V.; Grün, F.; Pinter, G.; Schwarz, T. Development of Ring on Disc tests for elastomeric sealing materials. In Proceedings of the International Tribology Conference, Tokyo, Japan, 16–20 September 2015.
30. Stevenson, A.; Shepherd, R. An overview of the requirements for seal life prediction Part 1—Static seals. *Seal. Technol.* **1995**, *13*, 9–12. [CrossRef]
31. *ASTM Standard D-471-06*; ASTM International: Conshohocken, PA, USA, 1998.
32. Shell Vitrea Oils, Premium Quality Industrial Oils. Available online: http://www.dayanoilco.com/upload/product/1451803762.pdf (accessed on 10 July 2017).
33. Base Oil Handbook, NYNAS. Available online: http://www.engnetglobal.com/documents/pdfcatalog/NYN001_200412073535_Base%20oil%20handbookENG.pdf (accessed on 3 August 2017).

34. Lv, X.R.; Wang, H.M.; Wang, S.J. Effect of swelling nitrile rubber in cyclohexane on its ageing, friction and wear characteristics. *Wear* **2015**, *328–329*, 414–421. [CrossRef]
35. Simmons, G.F.; Mofidi, M.; Prakash, B. Friction evaluation of elastomers in lubricated contact. *Lubr. Sci.* **2009**, *21*, 427–440. [CrossRef]
36. Lou, W.; Zhang, W.; Liu, X.; Dai, W.; Xu, D. Degradation of hydrogenated nitrile rubber (HNBR) O-rings exposed to simulated servo system conditions. *Polym. Degrad. Stab.* **2017**, *144*, 464–472. [CrossRef]
37. Yang, R.; Zhao, J.; Liu, Y. Oxidative degradation products analysis of polymer materials by pyrolysis gas chromatography mass spectrometry. *Polym. Degrad. Stab.* **2013**, *98*, 2466–2472. [CrossRef]
38. Zhao, J.; Yang, R.; Iervolino, R.; Barbera, S. Changes of chemical structure and mechanical property levels during thermo-oxidative aging of NBR. *Rubber Chem. Technol.* **2013**, *86*, 591–603. [CrossRef]
39. Sanches, N.B.; Cassu, S.N.; Dutra, R.C.L. TG/FT-IR characterization of additives typically employed in EPDM formulations. *Polímeros* **2015**, *25*, 247–255. [CrossRef]